

NASA CR-54108

N64-24845

Code 1
Cat.-06

56 P.

RESEARCH AND DEVELOPMENT
IN
CdS PHOTOVOLTAIC FILM CELLS

by

T. A. Griffin, R. W. Olmsted, J. C. Schaefer

prepared for

NATIONAL AERONAUTICS AND SPACE ADMINISTRATION

CONTRACT NAS 3-2493

OTS PRICE

XEROX \$ 5.60 ph
MICROFILM \$ _____

THE HARSHAW CHEMICAL CO.

FINAL REPORT

RESEARCH AND DEVELOPMENT
in
CdS PHOTOVOLTAIC FILM CELLS

by

T. A. Griffin, R. W. Olmsted, J. C. Schaefer

prepared for

NATIONAL AERONAUTICS AND SPACE ADMINISTRATION

May 29, 1962 to June 10, 1964

CONTRACT NAS 3-2493

Technical Management
NASA Lewis Research Center
Cleveland, Ohio
Space Power Systems Division
Clifford Swartz

Harshaw Chemical Company
Crystal-Solid State Division
1945 E. 97th Street
Cleveland 6, Ohio

FORWARD

The work of this project has been carried out at the Crystal-Solid State Research Laboratory of The Harshaw Chemical Company. Dr. J. M. McKenzie is the technical director of the laboratory. The work was sponsored by the Lewis Research Laboratory of NASA with Dr. Andrew E. Potter acting as technical advisor, and Clifford Swartz acting as Project Manager. Project direction has been provided by Mr. F. A. Shirland and Mr. J. C. Schaefer. Mr. T. A. Griffin has acted as the Project Supervision Engineer and Principal Investigator.

The following Harshaw Chemical Company personnel have contributed to this program: R. W. Olmsted, W. W. Baldauf, D. D. Bell, D. H. Dickey, R. F. Belt, and R. J. Humrick.

TABLE OF CONTENTS

	<u>PAGE</u>
SUMMARY	1
INTRODUCTION	2
CELLS DELIVERED ON CONTRACT	4
EVAPORATION EQUIPMENT MODIFICATIONS	4
Filaments	4
Substrate Heater & Holder	5
EVAPORATION MATERIAL	8
Microscopic Analysis	8
Spectrographic Analysis	9
X-Ray Analysis	11
EVAPORATED FILMS	13
Uniformity	13
Electrical Properties	13
WEIGHT REDUCTION	15
Substrates	17
Molybdenum	17
Invar & Kovar	17
Tungsten	17
Niobium	17
Zirconium & Tantalum	19
Silver & Zinc	19
Titanium	19
Film Thickness	19
CDS-SUBSTRATE CONTACT	20
CELL TESTING	24
I-V CURVE ANALYSIS	25

TABLE OF CONTENTS (Continued)

	<u>PAGE</u>
COLLECTOR ELECTRODE	30
Sheet Resistance	31
Electroforming	40
CELL ENCAPSULATION	41
Plastics	43
Encapsulation	43
Miscellaneous Improvements	44
Lead Attachments	44
PILOT LINE	45
REFERENCES	48

LIST OF FIGURES

<u>FIGURE</u>	<u>TITLE</u>	<u>PAGE</u>
1	Filament Arrangement for 6" x 6" Film Evaporation	6
2	6" x 6" CdS Front Wall Solar Cell	6
3	Substrate Heater and Holder	7
4	Bulkhead Feedthroughs for Substrate Heater	7
5	Curves of Power Versus Load Resistance	26
6	Actual and Calculated I-V Curves	28
7	I-V Curve at Three Light Intensities for Estimation of Series Resistance	29
8	I-V Characteristic Curves for Cell X-114 with Different Collector Grids	32
9	Electrical Test Circuit for Measurement of Barrier Sheet Resistance	33
10	Circuit to Explore the Potential Distribution of Cells .	39
11	Rear Wall Cell Fabricated by Etching Substrate	42
12	Pressure Test Unit Diagram	46

LIST OF TABLES

<u>TABLE</u>	<u>TITLE</u>	<u>PAGE</u>
I	Quantitative Spectrographic Analysis of CdS Material	10
II	X-Ray Data for Thin CdS Films	12
III	Properties of CdS Films Evaporated at Various Substrate Temperatures	14
IV	Properties of CdS Films Evaporated from Various Starting Materials	16
V	Properties of Possible Metal Substrate Materials	18
VI	Typical Values for CdS "n" Type Contacts to Various Substrates and Interface Materials	23
VII	Comparison of Various Meshes as Collector Electrodes	34
VIII	Mesh Collectors from Table VII Listed According to Efficiency	35
IX	Barrier Sheet Resistance Measured with Cells in Various Ambients and after Various Treatments	37

RESEARCH AND DEVELOPMENT

IN

CdS PHOTOVOLTAIC FILM CELLS

by T. A. Griffin, R. W. Olmsted, and J. C. Schaefer

24845 SUMMARY

ABSTRACT

This CdS thin film solar cell program has materially contributed toward an increase in the watts per pound, cell size, and an improved cell package. It has also produced an increase in the cell efficiency by means of an improved collector and has shown a method for possibly improving said collector by electrodeposition. A large number of various sized cells has also been delivered for a great variety of environmental tests. Cell cost reductions have been effected.

Work has been accomplished on cell series resistance, crystallite size, and evaporant powders.

AUTHOR

RESEARCH AND DEVELOPMENT
IN
CdS PHOTOVOLTAIC FILM CELLS

by T. A. Griffin, R. W. Olmsted, and J. C. Schaefer

INTRODUCTION

The cadmium sulfide solar cell program was initiated at Harshaw about ten years ago by the United States Air Force. Since then it has been augmented by the National Aeronautics and Space Administration. The purpose of this National Aeronautics and Space Administration program was to concentrate on certain aspects of the CdS film cell design so that it might become more competitive with existing space power systems. The cell development has progressed to the threshold of serious consideration for space power.

To reach this point, the power to weight ratio and the energy conversion efficiency had to be increased. Reliability had to be designed into the cell package. Substantial advances were made in these areas.

Several important developments were made during this contract. One was the fabrication of six inch by six inch solar cells, which are probably the largest individual units ever made. Another important milestone was doubling the cell output by employing an electroformed gold grid collector. The successful employment of a very light weight metal substrate, e.g., titanium, and the increased reliability of the cell package were other improvements.

Advances were also made in lowering the cost of these cells. Electroplated grids show promise as replacements for the expensive electroformed meshes. The evaporant, originally single crystal chips, is now raw powder. A large number of cells of various sizes were produced ranging from 1 cm x 2 cm to the 6 inch x 6 inch cells. A substantial number of these were sent to the National Aeronautics and Space Administration for testing and evaluation.

It is expected that the results of these tests will indicate further improvements especially in the cell package design.

The established radiation resistance, the constantly improving efficiency, the high power to weight ratio, and the low cost make the thin film CdS flexible solar cell the brightest prospect in the solar cell field.

CELLS DELIVERED DURING CONTRACT

During this solar cell contract over 300 cells were delivered to the National Aeronautics and Space Administration. These cells were fabricated to demonstrate the state of the art, and to be used in performance tests. A few general comments can be made concerning these cells.

Among these cells seventeen 6" x 6" cells are the largest known individual solar cells ever made. Figure 2 is a photograph of typical 6" x 6" cells. Eight 6" x 6" arrays were also fabricated from four individual 3" x 3" cells connected in series or parallel and laminated in one package. One hundred forty-six individual 3" x 3" cells were delivered along with one hundred thirty-eight 1 x 2 cm cells. Several dozen mechanical samples of different sizes were constructed for various purposes. The majority of the above cells were front wall cells fabricated on flexible substrates.

Most of the cells were over 2.5% efficient with several over 3%. The highest efficiency large area cell delivered was 3.52%. However, higher efficiencies are now being attained. The highest power-to-weight ratio demonstrated in these cells was twenty-eight watts per pound. The grid area was used to calculate efficiencies. Cells were tested under tungsten lamps.

Many of these cells are being used in an environmental test program now in progress at the National Aeronautics and Space Administration, Lewis Research Laboratories.

EVAPORATION EQUIPMENT MODIFICATION

The object of modifying the evaporation equipment was, not only to provide more uniform CdS films, but also to produce larger films. Even though a 6" x 6" area was chosen, it does not mean that this is the optimum cell size. If films of thirty-six square inches could be handled, then the only limit on area would be chamber size and filament position. To achieve these goals the filament, the substrate heater, and the substrate holder designs were studied and modified.

Filaments

A tantalum filament developed for the evaporation of SiO was first evaluated. ⁽¹⁾ SiO and CdS both vaporize without going through the melt phase. Precautions must be taken to eliminate splatter caused by small unvaporized particles that get blown off of the surface of the charge as it vaporizes. This filament was designed to force the vaporized material to enter a chimney through small holes. The vapor exits through the top of the chimney and is directed to the substrate. Thus particles must pass through the small holes, and then make a 90° turn before striking the substrate and causing pin holes in the evaporated film. This effectively prevents the impingement of small unvaporized particles on the substrate, and reduces pin holes and splattering.

In evaluating this filament it should be pointed out that it provided high evaporation rates, and produced little splatter. However, the evaporation rate was not constant and depended on the amount of charge remaining in the filament. To approach uniformity over 6" x 6" areas it was necessary to use a very large substrate-to-filament distance. This resulted in much wasted evaporant. In spite of the large separation of filament and substrate, the evaporated films were still not very uniform. The variation over the 6" x 6" areas was in excess of 30%.

Therefore, from the above experiences, and because the SiO filament had a limited life, another filament type seemed necessary.

A group of four filaments was found adequate for the evaporation of CdS on a 6" x 6" substrate. This design permits adjustment of the filament positions to give a uniform deposit over the 6" x 6" substrate area. The filaments are constructed of tantalum cylinders $\frac{1}{2}$ " in diameter, and $3\frac{1}{2}$ " long. The basic procedure used for achieving uniformity over large squares is to place the filaments on centers equal to the substrate sides, in this case on 6" centers, then the substrate to filament distance is adjusted to 75% of the six inches.⁽²⁾ This basic method did not hold true here because the filaments served as collimated sources. Therefore, the final distances were adjustments made by trial and error. The four filaments are positioned on 4" centers, while the best substrate to filament distance is 9.2 inches. Figure 1 shows the filament configuration with the heat shields removed for easier viewing.

The filaments are wired in series to enable the changing of individual filaments without disturbing the other three. Most importantly, the line drop is minimized, thereby permitting the power to be more efficiently coupled to the filaments. It has been found that only about one-half of the originally estimated power, or a little more than 2 kw is required.

In order to conserve power and also reduce the heat radiated to the bell jar, tantalum reflectors or shields were installed adjacent to the filaments.

To minimize the splattering, quartz wool plugs were placed in the open end of the filaments. These plugs were effective in reducing the splattering. There was a reduction in the evaporation rate and the film thickness.

The quartz wool plugs are not quite adequate when used alone. Etched screens of five mil molybdenum are used as caps to hold the charge in the boat. These caps are attached to the heat shields mentioned above. This procedure has effectively eliminated the splatter. Since this development, raw power is being used as an evaporant.

Substrate Heater and Holder

Originally the substrates were heated by radiation by means of a molybdenum strip resistance heater placed just above the substrate. The heat transfer was not as efficient as desired and a new heater design was sought.

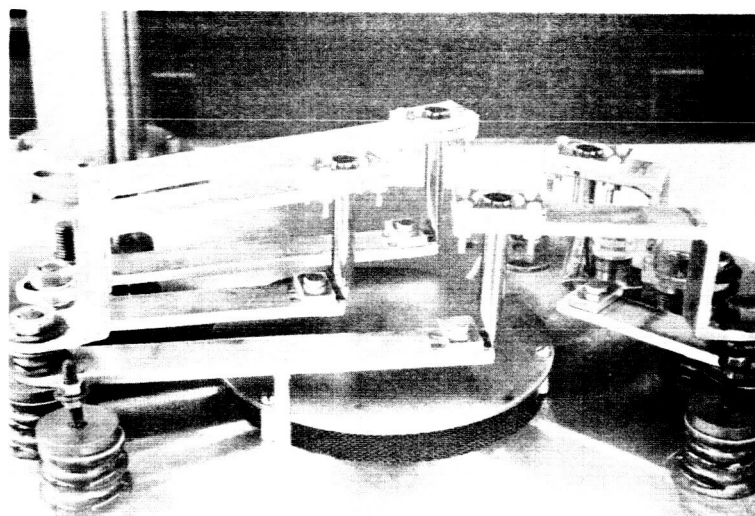


FIGURE 1

FILAMENT ARRANGEMENT FOR
6" x 6" FILM EVAPORATION.

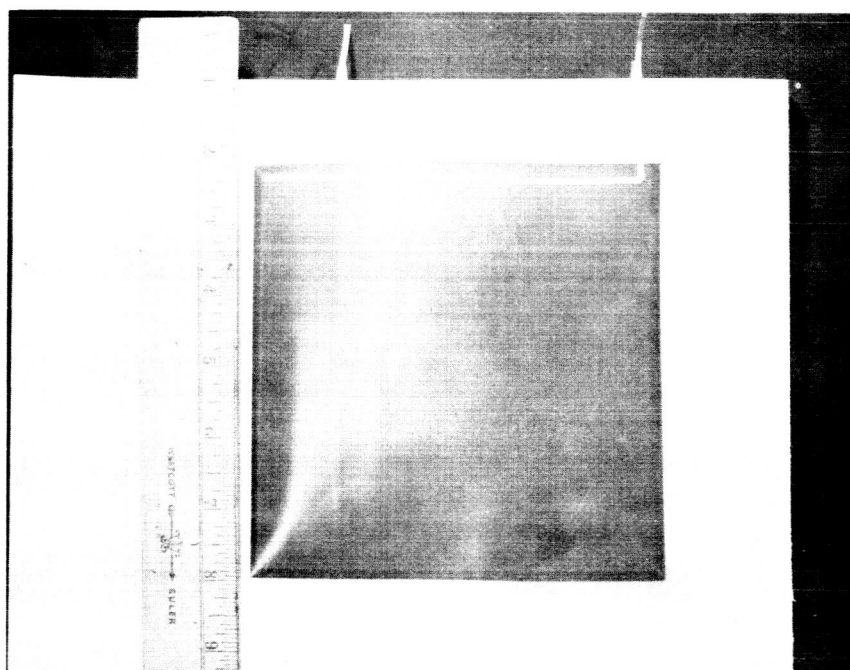


FIGURE 2

6" x 6" CdS FRONT WALL
SOLAR CELL



FIGURE 3
SUBSTRATE HEATER AND HOLDER.

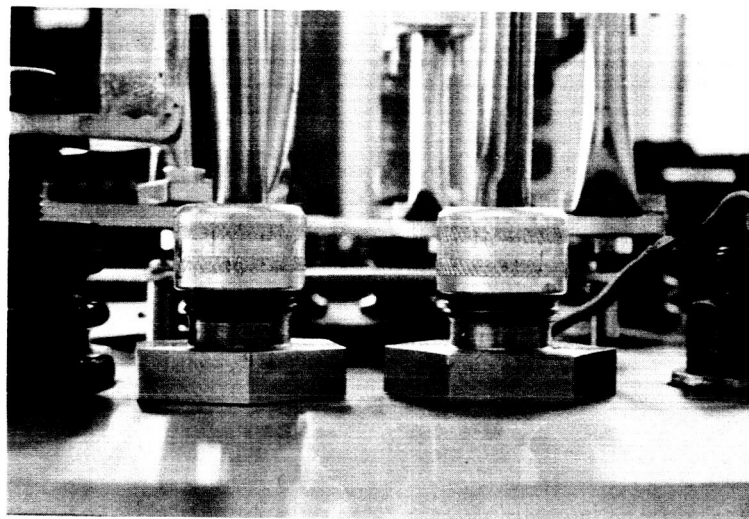


FIGURE 4
BULKHEAD FEEDTHROUGHS
FOR SUBSTRATE HEATER.

In an attempt to obtain more uniform heating of the substrate, several experiments were made using the substrate to supply its own heat by passing current through it. This did not prove successful because the contacts at the edges of the large substrates acted as heat sinks producing an unwanted temperature gradient across the substrate. This was compensated for by tailoring the geometry of the substrate. However, this proved so inaccurate that another substrate heater was developed.

The heat source chosen was an immersion heater enclosed in an incology sheath. (3) Figure 3 shows the final design of the substrate heater and holder. The heater was formed into an 11" diameter circle parallel to the base plate. The major length ($27\frac{1}{2}$ " of the 33" circumference) of this circle contains a 1.5 k.w. heater. The cold ends of the heater are $28\frac{1}{4}$ " tubes, which act as the vertical supports, and feed-throughs for the base plate. The bulkhead seals are made with flexible conduit seals which can be seen in Figure 4. As a result of this construction, the substrate heater is both self-supporting and adjustable in height.

Figure 3 shows the substrate heater clamped tightly to the substrate holder which is a $\frac{1}{4}$ " aluminum plate with a 6" x 6" square hold in the center. The substrates, which are slightly larger than 6" x 6", cover the opening and are backed with another aluminum plate. The back-up plate is also bolted to the substrate holder. In order to improve the heat transfer, the back of the substrate and the front of the back-up plate are covered with a black dag. Initially, because of the difference in the thermal expansion of the molybdenum substrate and the aluminum holder, some buckling was produced in the substrate during evaporation. It was discovered that the buckling could be completely eliminated by using a graphite coating between the substrate and the substrate holder. This allows the two metals to slide against each other during expansion and contraction.

This substrate heater is much more efficient than the radiation type. It requires about one-fourth the amount of power to heat the substrate to a given temperature.

EVAPORATION MATERIAL

Microscopic Analysis

When the evaporated CdS film cell evolved from the CdS single crystal cell the material used as an evaporant was single crystal chips. Subsequently it was discovered possible to use sintered polycrystalline material as an evaporant. Now, raw powder has been found to be suitable. Powder supplied by several manufacturers has been tried, but only the General Electric material has been handled satisfactorily by the present filaments. With other materials there was considerable splattering on the films. This splattering is due to grain size as is shown in the following comparison. The grain sizes as found by microscopy were:

General Electric Powder:

Range = less than 1 micron to 3 microns

TABLE I

QUANTITATIVE SPECTROGRAPHIC ANALYSIS OF Cds MATERIAL

	G.E. POWDER (ppm.)	SYLVANIA POWDER (ppm.)	MERK POWDER (ppm.)	EAGLE PITCHER POWDER (ppm.)	SINTERED G.E. POWDER (ppm.)	SINGLE CRYSTAL FROM G.E. POWDER (ppm.)
Aluminum	<2.0	2.3	6.0	3.0	<2.0	4.3
Calcium	1.7	1.5	>50.0	2.0	2.1	2.2
Copper	<1.0	2.4	1.1	2.0	<1.0	1.0
Indium	<1.0	1.2	<1.0	2.0	1.1	2.6
Iron	<2.0	<2.0	<2.0	<2.0	<2.0	<2.0
Magnesium	<1.0	1.2	2.5	2.0	<1.0	<1.0
Manganese	-	-	-	-	-	-
Nickel	-	-	-	-	-	-
Silicon	<2.0	6.2	3.5	4.0	2.0	10.0
Thallium	-	-	-	-	-	-

evident that there are no significant differences in impurities for the various materials. Both the sintered material and the single crystal material were made using the General Electric powder as a starting material. Certainly, because of the complete dissociation that occurs in the evaporation process, and the vapor pressures present, some further purification occurs during film deposition.

X-Ray Analysis

Thin films of the materials were deposited by use of the standard evaporator. The geometry of the vapor source, the substrate, and their respective heaters were similar to that previously reported. Efforts were made to keep evaporating techniques constant. The purpose of the experiments was to determine what changes in film structure, if any, could be attributed to the CdS source material. If noticeable effects are absent, several forms of CdS are suitable for evaporating films. A priori, CdS should evaporate and deposit in a manner which is independent of preparation. However, differences in impurity content, particle size, and other chemical or physical properties, may effect changes in the deposited films.

Films of the various CdS sources were evaporated on glass and molybdenum substrates which in turn were studied by x-ray techniques. For each evaporation onto molybdenum a glass substrate was included so that the film on the glass could be used for resistivity and Hall measurements. The films on molybdenum were used later for cell fabrication.

After the evaporated CdS films were prepared, they were examined by x-ray procedures for lattice spacing changes, orientation, and relative crystallite size. The data have been assembled in Table II. It may be noticed that the d spacings of the (002) planes are constant at $3.359 \pm 0.01\text{\AA}$. The (002) planes are nearly parallel to the substrate and small differences in spacings may be caused by film thicknesses, strain, measurement error, and defect content. No specific data can be correlated with the source alone. The peak intensity of (002) is measured in a number of planes, or crystallites oriented parallel to the substrate. Many variables can change this orientation. The General Electric sintered powder evaporated on glass substrates appears to give the best orientation. However, this could be fortuitous. It is known that biaxial orientation occurs in CdS films. More complete pole figures are needed to confirm the results. The width at half maximum for (002) may be taken as an indication of crystallite size in a direction perpendicular to the substrate. Larger widths correspond to small crystallite sizes. Here again the range of observed widths is quite scattered. Definite correlations are difficult to form.

The widths are also influenced by strain and other defects which are always present in the films. In conclusion, the limited data given here shows no outstanding differences which may be attributed to the original source of the CdS.

TABLE II
X-RAY DATA FOR THIN Cds FILMS

COMMERCIAL SOURCE	SAMPLE NO.	SUBSTRATE	θ d in A of (002)	PEAK INTENSITY OF (002) cp	WIDTH AT HALF MAXIMUM FOR (002) (2°)
General Electric Sintered	X580	Pyrex	3.359	49,500	.191
General Electric Sintered	51	Glass	3.364	75,000	.238
General Electric Sintered	57	Glass	3.359	100,000	.238
General Electric Sintered	74	Glass	3.368	68,000	.172
General Electric Sintered	73	Glass	3.365	65,000	.203
General Electric Sintered	47	Glass	3.362	5,760	.215
General Electric Sintered	47	Mo	3.354	40,000	.252
Sylvania Powdered	54	Glass	3.362	4,000	.195
Merck Powdered	53	Mo	3.358	22,600	.203
Merck Powdered	53	Glass	3.359	35,000	.211
Eagle-Pitcher Powdered	X588	Pyrex	3.361	4,800	.164
Harshaw Single Crystal	X586	Pyrex	3.361	871	.218

EVAPORATED FILMS

Uniformity

To determine the thickness profile of the 6" x 6" films detailed measurements were made on two films. The first film had the CdS removed from the substrate at nine spots and the thickness was measured. The CdS thickness was found to vary from 1.5 to 2.1 mils. Then all of the CdS film was removed, collected, and weighed. On the basis of total weight and the area covered, the thickness was found to be 1.7 mil. A second film had its deposit measured by using a microscope to determine the thickness of the CdS at the edges of several holes placed in the film. The thickness was found to vary from 1.7 to 2.1 mils by this method. Since these types of measurements are destructive, subsequent films were only checked with a surface gauge. The uniformity seemed reasonable and sufficient for the production of good films. About eight per cent of the total filament charge was collected on the substrate. If it is desired to collect more of the charge, the rate of evaporation must be increased. The explanation for this is described elsewhere.⁽⁴⁾

Electrical Properties

The electrical properties of the evaporated CdS films were examined. These properties included resistivity, mobility, and carrier concentration. An attempt was made to relate these properties to substrate temperature, starting material, and cell operation.

A series of evaporations were run at various substrate temperatures to see what effect this has on cell operation. Table III shows the results of this series. The standard substrate temperature, at this time, was approximately 220°C. Most of the films formed or condensed at this substrate temperature had resistivities in the 10^3 ohm-cm range.

First, it should be pointed out that the material evaporated is undoped CdS. Therefore, any variations in resistivity probably comes from non-stoichiometry. This is evident in the low resistivity films achieved by evaporation at low substrate temperatures. These films are very dark in appearance which indicates a large cadmium excess. It is of interest that the substrate temperature normally used (220°C) gives the highest resistivity films. However, it also appears to give cells with high current density. In this particular series 250°C yielded better cells. Subsequent tests have shown 220°C is a slightly better temperature. However there seems to be a range of 25 or 30°C that yields very similar results.

Pertinent to this question are some series resistance calculations made on CdS film cells. The I-V curves of the 6" x 6" cells show a series resistance of about 0.1 ohm while the 1" x 3" cells show about 1 ohm. Comparing the two sizes on a basis of area and thickness, the bulk resistivity of the CdS film could be the cause of this series resistance. Calculations for the one ohm series resistance of one particular 1" x 3" cell resulted in a bulk resistivity of 3×10^3 ohm-cm; while the one-tenth ohm

TABLE III

PROPERTIES OF CdS FILMS EVAPORATED AT VARIOUS SUBSTRATE TEMPERATURES

SUBSTRATE TEMP. (°C.)	RESISTIVITY (in dark 1 hour) (ohm-cm)	RESISTIVITY (in light 150ft candles) (Ohm-cm)	CELL NO.	OCV (Volts)	SCI (ma.)	EFF. (%)
140	375	200	X479	0.42	12	N.C.*
			X480	0.5	58	1.3
180	650	340	X476	0.48	36	0.8
			X477	0.51	65	1.1
220	5200	1300	X483	0.49	124	2.2
			X484	0.5	116	2.4
250	1300	330	X471	0.52	124	2.8
			X472	0.52	120	2.6
260	850	230	X468	0.5	104	2.0
			X469	0.5	88	1.8

The material was the same for all films (Sintered CdS G.E. material, O-122)

Resistivity measurements were made on a pyrex slide that was evaporated at the same time as the film on molybdenum.

*N.C. = not calculated, very low.

series resistance on a 6" x 6" cell yielded a bulk resistivity of 5×10^3 ohm-cm. These films were evaporated at a substrate temperature of 220°C. As seen from Table III, bulk resistivities in the 10^3 ohm-cm range would be expected for the substrate temperature at which these films were evaporated. Whether this cell series resistance can be related to the bulk resistivity, or not, is to be determined. Further comment on this will be found later in this report.

The resistivity, mobility, and carrier concentration, were measured using films made from the various source materials. Table IV displays the results. The films from Sylvania powder seem to show the lowest resistivity. However these films had so much splatter that the thickness measurement used in the calculation of resistivity was very inaccurate. The single crystals were doped in the 1 to 10 ohm cm. range and therefore the films have about the expected resistivity. The General Electric sintered material gave films with resistivities a factor of ten lower than the General Electric powder.

The mobilities are in the expected range. The one exception is the Eagle Pitcher material which gave films of high mobility.

No significant differences were noted in open circuit voltages, or short circuit currents for any one group of cells from the same material.

One property that did vary was the shunt resistance. To evaluate this property the value of shunt resistance obtained from the I-V curves was multiplied by the cell area since the cell areas varied from 12 cm² to 210 cm². This normalized value of shunt resistance ranged from 100 ohm cm² to 31×10^3 ohm cm². It is felt that this great variation is due to the film structure, and in particular to the partial shorting paths such as pin holes, grain boundaries, etc.. There was no correlation between shunt resistance and source material.

The series resistance is of special interest since a decrease of this property would mean an immediate increase in cell efficiency. As mentioned above, there appeared to be some indications that cell series resistance might be correlated to the bulk resistivity of the film. However, after the values were adjusted by using the cell areas to obtain a common figure, no correlation was evident. The series resistance varied from 6 to 25 ohm cm². The film resistivities ranged from 0.6 ohm cm to 14×10^3 ohm cm. If much of the series resistance of the cell is due to the bulk resistivity of the film, it will be very hard to separate it from the total series resistance.

WEIGHT REDUCTION

One of the advantages of the flexible front wall CdS solar cell over present solar cells is its light weight. Even though the efficiency of CdS film cells has not exceeded 5.5%, they are lighter than high efficiency cells and can deliver more power per unit of weight. Thirty watts per pound has been demonstrated several times on large area cells. This ratio can be increased in many ways. The most obvious way is to reduce the overall weight

TABLE IV

PROPERTIES OF CDS FILMS EVAPORATED FROM VARIOUS STARTING MATERIALS

MATERIAL	SAMPLE NO.	THICKNESS MILS	RESISTIVITY OHM CM	MOBILITY CM ² /V. SEC	CARRIERS CM ⁻³
General Electric Sinter	57	1.1	28	0.55	4.8×10^{17}
General Electric Sinter	51	1.8	--	--	--
General Electric Sinter	74	1.5	27	0.4	6×10^{17}
General Electric Sinter	X579 X580 X581	2.0 2.0 2.0	16	1.9	2.5×10^{17}
General Electric Powder	47	1.7	560	--	--
General Electric Powder	77	1.6	270	<0.1	5×10^{16}
General Electric Powder	80	1.0	1200	--	--
General Electric Powder	82	1.5	1400	0.7	1.5×10^{16}
Sylvania Powder	49	1.2	0.6	1.5	8.5×10^{18}
Sylvania Powder	54	0.5	--	--	--
Eagle Pitcher Powder	X588 X589 X590	1.3 1.3 1.3	240	3.9	7.9×10^{15}
Harshaw Single Crystal	X585 X586 X587	1.5 1.5 1.5	4.6	3.7	4.3×10^{17}

by reducing the substrate weight and the CdS film thickness.

Substrates

When the CdS polycrystalline film cell was first reduced to practice it was found that fairly thick films in the order of 2 to 4 mils were required. To promote adherence it was believed that evaporated films would have to be laid down on substrates that closely matched the thermal expansion of CdS. For this reason, the first rear wall film cells were made on pyrex glass substrates. The first front wall film cells were made on molybdenum substrates. Both of these substrate materials match CdS closely in thermal expansion coefficient. Several metals have been used or considered for substrate materials. Table V lists these materials and their properties.

1. Molybdenum

Two mil molybdenum has been used for most of the front wall CdS film cells produced thus far. One mil molybdenum has been substituted for the two mil molybdenum in the past, but it presents problems. Care must be taken to avoid any kinks or folds in the foil during processing. The most serious problem in preparing one mil molybdenum for large area substrates is the condition of the material as supplied. Much of the material is already full of dents and folds. Recently evidence has been accumulated that the thin foil does not etch in the same manner as the two mil foil. This seems to indicate that the interface between the CdS and the molybdenum is different for the two thicknesses.

2. Invar and Kovar

Some Invar "36" has been used as a substrate material. Very little curling was noted in the cells, indicating a minimum of thermal expansion mismatch between the CdS and the Invar. Some very excellent cells, over 3.5% have been produced on this substrate, however, the yield has been very low. Most of the time the cells are poor, or the adhesion has not been satisfactory. One problem has been the etch rate. The reaction of Invar with HNO_3 and with HF is erratic. The rate of reaction with one test piece may be twice that of another piece. This makes it difficult to formulate an etching procedure for the metal. The reason for this variation in rates is being studied. Kovar has been found to be very similar to Invar. Both Kovar and Invar have the drawback of being magnetic which would rule out their use on a scientific satellite.

3. Tungsten

Good cells have been produced on two mil tungsten. Although the thermal match between CdS and tungsten was better than that between CdS and molybdenum, the tungsten is very dense, 19.3 g/cm^3 .

4. Niobium

Niobium produced by ordinary rolling and by Sendzimir processing

TABLE V

PROPERTIES OF POSSIBLE METAL SUBSTRATE MATERIALS

Material	Coefficient of Thermal Expansion ($^{\circ}\text{C} \times 10^{-6}$)*	Electrical Resistivity (Micro-ohm cm)	Density (g/cm ²)
Mo	4.7 to 5.8	5.2	10.2
Invar "36"	1.2 to 4.9**	82.0	8.1
Invar "42"	4.6 to 4.9**	72.0	8.4
Ag	20.2	1.6	10.5
Ta	6.6	12.4	16.6
Zr	6.1	4.5	6.5
Ti	9.4	47.8	4.5
W	4.6	5.5	19.3
Nb	7.5	13.1	8.6
Zn	34 to 39	6.0	7.1
V	7.8 (from 0 to 40 $^{\circ}\text{C}$)	24.8	6.0
CdS (11)	4 (at 25 $^{\circ}\text{C}$)		
CdS (1)	6 (at 25 $^{\circ}\text{C}$)		

* Over the range 20 to 300 $^{\circ}\text{C}$, except where otherwise noted.

** Values supplied by manufacturer. Other materials as listed in Amer. Inst. of Physics Handbook (1957 Ed.)

has been used. No cleaning, etching, or surface conditioning has been discovered that will promote the adherence of the CdS.

5. Zirconium and Tantalum

Zirconium and tantalum have been worked with, but with little or no success. The problem seems to be the removal and prevention of reformation of the film that forms on the surface of these metals. The adherence to these metals is very poor.

6. Silver and Zinc

Some metals can be used successfully even though they do not match the thermal expansion of CdS provided they are soft or fairly ductile.

Good cells have been made on both one mil zinc and one mil silver. The adherence of the CdS was not as good as it was to molybdenum, but it was sufficient to enable the fabrication of several cells.

7. Titanium

Titanium is of interest because of its very low density (4.5 g/cc). Until recently titanium was in the same class as zirconium and tantalum. Now an etch method has been developed for titanium that is reasonably successful. It is not the ultimate answer.

The etching of a metal to be used as a substrate should do two things; first, clean it, and second, roughen the surface. It would also seem desirable that the surface be uniformly etched, although this is not always essential. The surface should be free from all contaminants and oxides so that the CdS can bond well to it. The amount of roughening necessary is hard to gauge. Usually a great deal is not any better than a moderate amount. Aside from these points, there is no other criterion for deciding when a surface is well etched. In the final analysis it is the adherence to the CdS that determines whether the surface preparation is adequate.

Film Thickness

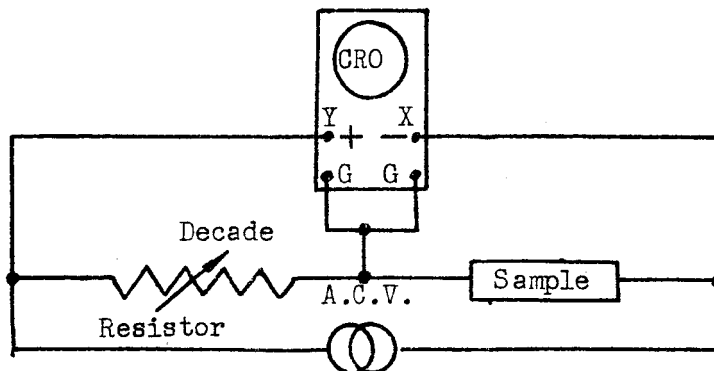
As stated above, one method of increasing the power-to-weight ratio of thin film photovoltaic cells is to decrease the weight of the cells. A great part of the weight of the CdS thin film cell is in the substrate. However, it has been found that molybdenum and other metal foil substrates, when reduced in thickness, give excessive curling of the CdS film-substrate combination. In order to minimize the curling, the CdS film and metal substrate must be approximately the same thickness.

Thus, the key to higher watts per pound by lighter weight construction seems to be the successful use of thinner CdS films. At first, very thick CdS films, in the range of 0.003" to 0.005", were needed because thinner films gave excessive shorting between the barrier and the substrate. As

improved vacuum evaporation procedures, and improved methods of cleaning the substrates were developed, the CdS film thickness was successfully reduced to approximately one mil. The most important factor in making films of this thickness suitable for cells is the elimination of splatter which causes pin holes. With the present state of the art it appears that one mil CdS is about as thin a film that can be made into a good solar cell. Most likely the limiting factor is the barrier formation method. Recently a new and higher efficiency barrier method⁽⁵⁾ has been developed that does not employ electroplating. It is hoped that this new barrier will be equal or superior to the electroplated barrier in regard to lifetime, radiation resistance, moisture degradation, etc; and will soon supplant the electroplated barrier. If this is accomplished, it is certain that thinner films of CdS can be used.

CdS-SUBSTRATE CONTACT

The film cell displays some series resistance that is not due to the collector electrode, but is in the barrier, in the bulk material, or in the contact between the "n" type CdS and the substrate. It was decided to first examine the latter area. The method employed was to make certain that an ohmic contact could be made to the CdS, and then the contact of the CdS to the metal substrate would be examined. After some data was accumulated on the ohmicity of the contact between CdS and various substrates, an effort was made to relate these contacts to cell operation and efficiency. The general pattern of testing involved applying circular indium-mercury amalgam⁽⁶⁾ electrodes (2 mm diameter) to the surface of the CdS film. The other terminal in these measurements was either the substrate or another In-Hg spot. The I-V curve of these two terminals was displayed by a standard circuit:

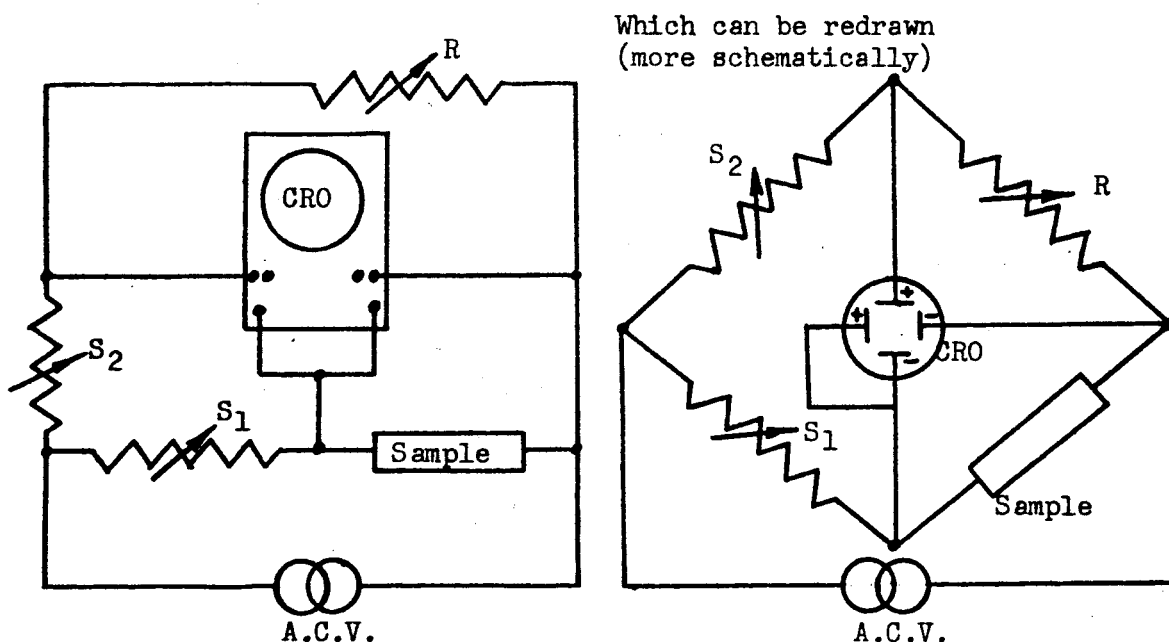


In order to accumulate further evidence that the In-Hg electrode was ohmic to the CdS film, a portion of the film was removed from the molybdenum substrate and two of the In-Hg contacts were applied. It was found that flakes which cracked away from a typical substrate were too small to be practical for this purpose. Larger samples of films were freed from the substrate by using an evaporated Victawet film between the CdS and molybdenum. Thicknesses of 400 Å, 200 Å, and 100 Å of Victawet all facilitated removal of CdS when the film and substrate were immersed in water.

Two In-Hg electrodes on the "front" surface of a CdS flake had a linear I-V curve. Some curvature in the I-V trace was noticed at 0.3 V peak-to-peak between an electrode on the "front" of a flake and another electrode on the back of the flake (the back being the side toward the substrate).

When the electrodes are both applied to the back of the flake the I-V trace indicated two symmetrical non-ohmic contacts. Therefore it appears that, In-Hg gives an ohmic contact to the front side of a CdS film, but for some unknown reason gives a slightly non-linear contact to the backside. In the subsequent tests its use was confined to the front side.

To show up small non-linearities in the I-V curves of the CdS on different substrates a bridge circuit had to be used. (An illustration of this is shown below.)



The lower branch of this circuit (when $S_2 = 0$ and $R \rightarrow \infty$) is like the ordinary I-V circuit where the current is indicated by the voltage across S_1 in series with the sample. Here, S_1 performs a function analogous to that of an ammeter shunt. When S_2 is not equal to zero or infinity and R is not equal to zero or infinity, the upper branch is similar to the lower branch except that the sample is replaced by a variable resistor, R .

In the case when $S_1 \neq S_2$ and the sample is an ohmic (linear) resistor, then the trace on the scope will be a straight line whose slope depends on the value of R . In particular, the trace will be a horizontal line when the value of R equals the resistance of the sample. The slope of the I-V curve at the origin can be measured by setting R so that the corresponding portion of the bridge curve is horizontal. The slope of that portion of the I-V curve is then $\frac{1}{R}$. Even if $S_1 \neq S_2$, we can set up a situation similar to

that above by adjusting the ratio of R and S_2 properly.

Some of the substrates used in these measurements to determine the ohmicity to evaporated CdS were molybdenum, silver, gold, zinc, and invar. Some interface materials were also tried. These were thin films, 50 Å to 100 Å thick, evaporated on 0.002 molybdenum. The CdS was then deposited on the interface layer under the standard conditions.

The first contact measured was that of CdS to Mo. It was not completely linear. Table VI lists the series resistance, which is calculated from the slope of the small signal curve before the curving due to the non-linearity of the contact is reached. The range of the non-linearity is listed in peak-to-peak values.

As can be seen from Table VI, a CdS film with a zinc substrate and an In-Hg contact showed a linear I-V curve. In other important aspects such as thermal expansion, molybdenum substrates are superior to zinc substrates. The above situation suggested the use of a thin film of zinc between the molybdenum and the CdS.

Zinc films were applied to molybdenum substrates by vacuum evaporation in two thicknesses, 40 and 100 Å. Then CdS was evaporated on the zinc layer. In each case two of the experimental substrates were coated along with one of a standard substrate for control. One of each pair of the films with the intermediate layer was tested with an In-Hg contact. The other was processed into a cell along with the control film. Under best conditions, the 50 Å zinc layer gave an ohmic contact between the substrate and the CdS, and raised the cell efficiency. Occasionally, the zinc intermediate layer yielded a black CdS layer. This darkening is found in some instances when CdS is evaporated on solid zinc substrates. The thicker zinc interlayer film had approximately three times the resistance of the thinner one. The reason for this is not known, but it may lie in the wide experimental errors involved.

Indium, cadmium, and tin were also tried as an intermediate layer. The results were less encouraging. In the spot tests, they gave non-ohmic contacts between the substrates and the CdS films. As with the zinc interlayers, these gave widely varying resistance values for the two different thicknesses, but usually much higher than was measured for zinc.

The cells fabricated from these films with various intermediate layers gave widely varying outputs and no clear indication pro or con could be obtained from the data. Quite a number of such cells were processed and it now appears likely that an evaporated intermediate metal layer is inherently too variable in quality under the CdS evaporation conditions to give consistent results.

Some films on the Invar "36" substrates had ohmic contacts, and some had non-ohmic contacts. The low signal resistance of the CdS-Invar contact was usually slightly less than that of the zinc coated molybdenum substrate films.

In summary, certain conclusions can be drawn from the above experiences.

TABLE VI

TYPICAL VALUES FOR CdS "n" TYPE CONTACTS TO
VARIOUS SUBSTRATES AND INTERFACE MATERIALS

Substrate or Interface Material	Resistance from Small Signal Slope	Range of Non-linearity
Mo	1.5 ohms	0.2 volts(p-to-p)
Zn	0.3	linear
Ag	2.4	0.2
Invar "36"	2.0	fairly linear
⁰ 50Å Zn or Mo	2.8	linear
⁰ 50Å In or Mo	27.0	0.1
⁰ 50Å Sn or Mo	1000.0	0.05
⁰ 50Å Cd or Mo	50.0	0.1
⁰ 100Å Zn on Mo	8.3	fairly linear
⁰ 100Å In on Mo	6.0	0.05
⁰ 100Å Sn on Mo	40.0	0.1
⁰ 100Å Cd on Mo	100.0	0.1

The substrate materials that gave ohmic or nearly ohmic contacts to CdS seemed to produce very slightly better photovoltaic cells. However, there is no indication of two opposed junctions in any of the I-V curves of the cells themselves, and since the non-linearities measured were very small, it seems probable that the contact (at least in the cases measured) had little effect on cell efficiency. The series resistance due to the contacts was so small when calculated over a large area that it was concluded that the CdS to substrate contact is not a very great factor in cell operation.

CELL TESTING

The CdS cells are tested by using the circuit found in the section on CdS-substrate contact. The light source is one or several RFL/2 photoflood tungsten lamps. Light sources that exactly duplicate the sun are impossible to devise. For this reason the intensity of the tungsten lamp is set so that the cells tested under it give approximately the same result they would if tested in collimated sunlight. Cells are periodically tested in sun and under tungsten and the results are compared. Below is the data for two cells tested on different days.

CELL	LIGHT	MEASURED INTENSITY	OCV	SCI	EFFICIENCY
219MN	Sun	89 mw/cm^2	0.46v	99ma	1.54%
	RFL/2	195 mw/cm^2	0.47	105	1.53
159AN	Sun	92 mw/cm^2	0.49	500	3.66
	RFL/2	195 mw/cm^2	0.49	500	3.4

From these and other tests it appears that the simulated terrestrial sunlight facility is reasonably accurate. The fact that some cells show greater discrepancies under the tungsten lamp than others is attributed to the non-uniform response of these cells to various colors. Some cells show enhancements due to the combination of certain wavelengths.⁽⁷⁾ However the tungsten light seems to be as accurate as any available source for the simulated testing of CdS cells.

In order to get a larger and more accurate display of the I-V characteristics of the cells, an X-Y plotter was placed in operation. Circuits were provided to test the cells "passively" (using a varying external power source) and "actively" (using the cell to provide its own power across a varying load). These large graphs of the I-V curves have aided in studying shunt and series resistance since these values are calculated from the slopes of the characteristic curves. It has also made it easier to locate the maximum power points on the curves.

I-V CURVE ANALYSIS

For most of the cells produced to date, the point of maximum power on the I-V curve has been located by calculating the product, $I \cdot V$, at a number of points until a maximum value is found.

A method found useful by other investigators involves superimposing a family of hyperbolas of constant $P = IV$ on the I-V curve. That hyperbola which is tangent to the I-V curve corresponds to the highest power along the I-V curve, and the point of tangency is the maximum power point.

A quick and simple approximation of the optimum power point has recently been found. The lines $V = V_{oc}$ and $I = I_{sc}$ are constructed. A third line is drawn through the intersection of the first two lines and through the origin. Where this third line crosses the I-V curve is approximately the maximum power point. This line corresponds to a load resistance of magnitude V_{oc}/I_{sc} . While this method is approximate, it would be useful as a time saver where many cells were produced and data was to be accumulated to detect changes in efficiency e.g. on a production line.

For an accurate determination of maximum power P_m and optimum load resistance, R_o , of a solar cell under given conditions, a curve of power versus load resistance may be plotted from data taken from the I-V curve of the cell:

$$P = VI, \quad R = \frac{V}{I}$$

It would be useful if an equation of P as a function of R could be found analytically or empirically. For example, the equation might be used to determine how close an approximation V_{oc}/I_{sc} would be for R_o . It might be possible analytically to transform a simple equation like:

$$I = I_o(\exp(qv/kT) - 1) - I_L \quad (8)$$

into an equation of P as a function of R .

A brief evaluation was made of a practicality of finding such an empirical equation. A plot of P vs. R is shown in the solid curve of Figure 5. The possibility of testing hypothetical equations against this curve with the aid of Harshaw's research computer was considered. The experimental curve roughly resembles the curve of the expression $P = aRe^{-br}$. The computer was used to generate values of this hypothetical curve. That data is shown as the dotted curve in Figure 5. While this approach to the problem appeared to be worthwhile, emphasis had to be shifted to other more fruitful work.

It is of continuing interest to consider various equivalent circuit models for a solar cell. One model consists of a current generator shunted by a diode:

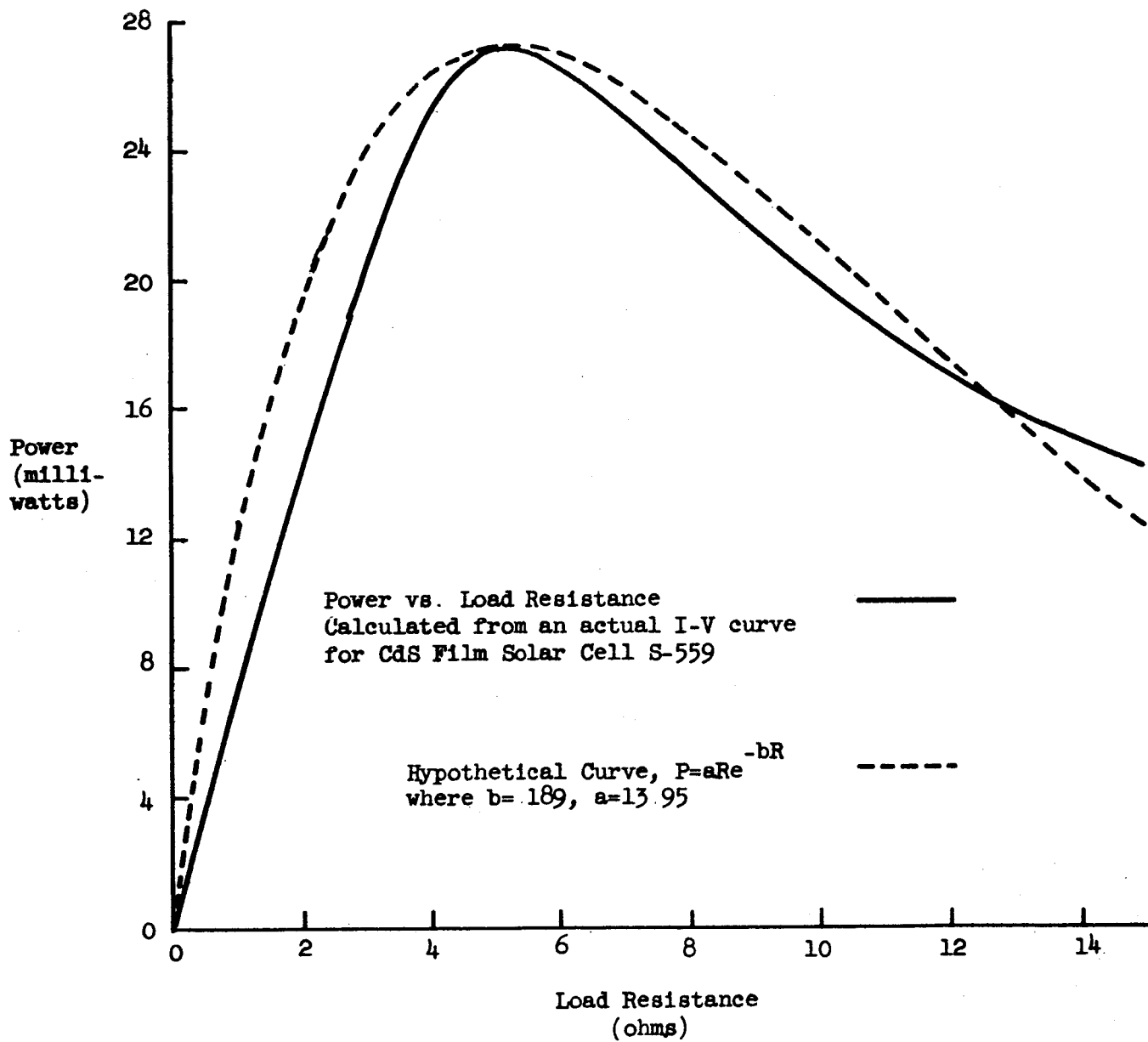
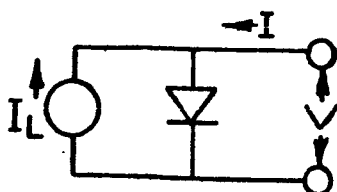


FIGURE 5
CURVES OF POWER VS. LOAD RESISTANCE



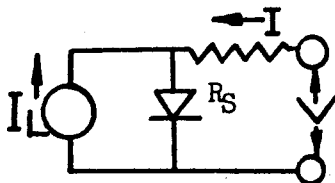
The output (I_L) of the current generator is a function (usually assumed linear) of the intensity of the light falling on the cell. The diode has an exponential characteristic, (saturation current, I_0). As a circuit element, the functional relationship of current (I) and voltage (V) of the model is given by:

$$I = I_0 (\exp (q V / A k T) - 1) - I_L$$

where q = the charge of the electron, k = Boltzmann's constant, T = the absolute temperature, and A is a parameter given as equal to unity by the early diffusion theory of the silicon cell.

At this laboratory⁽⁹⁾, it was found possible to "fit" curves of the above mathematical model to plots of experimental data obtained on cadmium sulfide solar cells (refer to Figure 6). The best fit of each curve was obtained using values from 3 to 4 for the parameter, A .

Another model adds a series resistance, R_s :



with the corresponding I-V relationship:

$$I = I_0 (\exp (V - I R_s) q / A k T) - 1) - I_L.$$

Where R_s has an appreciable effect on the I-V characteristic, its value can be estimated to be approximately equal to the reciprocal of the slope at the open circuit voltage intercept. Another way of estimating R_s involves taking experimental plots of the I-V characteristic of a cell at different light intensities.⁽¹⁰⁾ On the "knee" of each curve, a point is selected which has the same incremental difference in current from I_L , (refer to Figure 7). A straight line is fitted to the points and the reciprocal of its slope is chosen as an estimate of R_s .

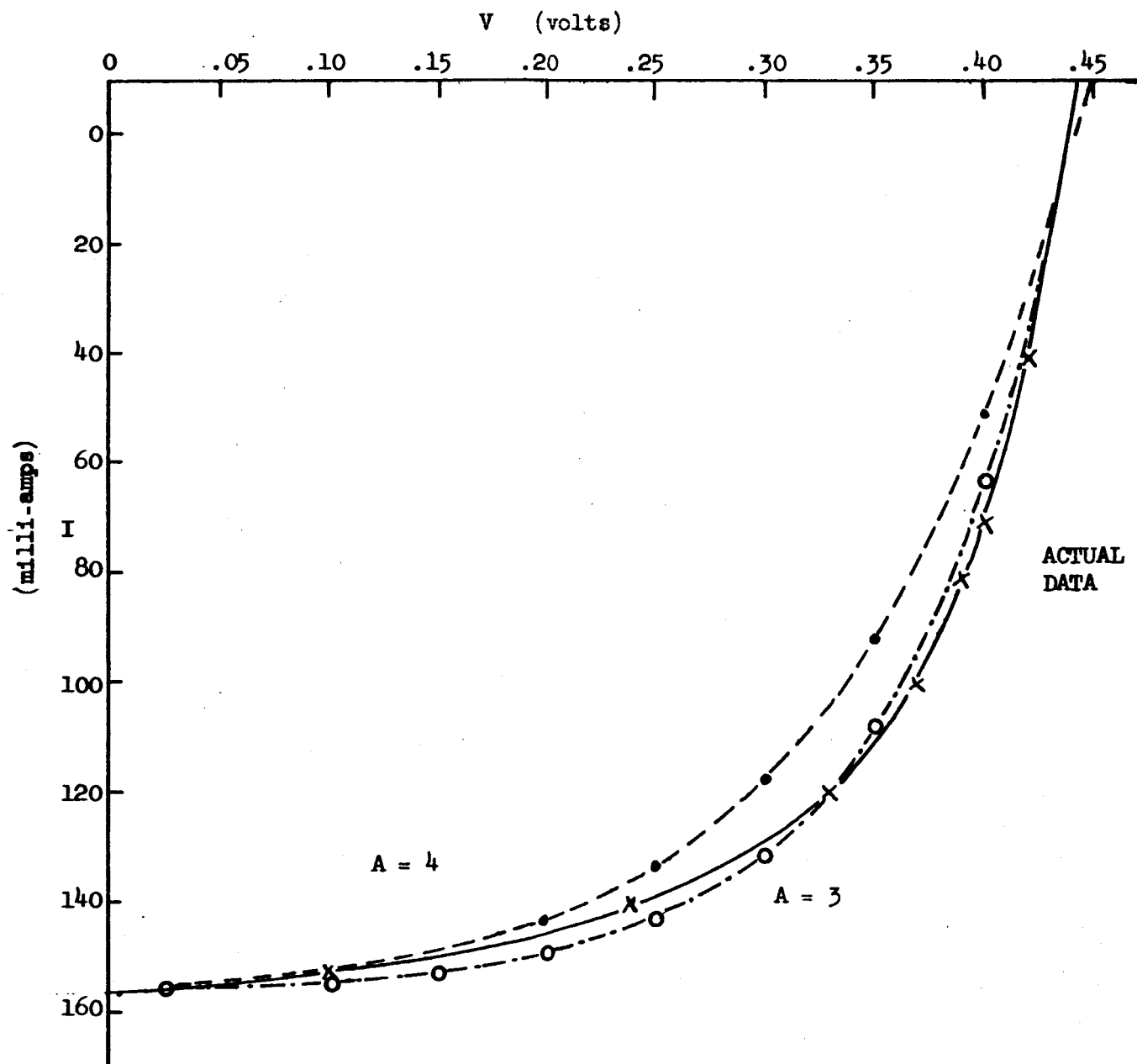


Figure
ACTUAL and CALCULATED I - V CURVES

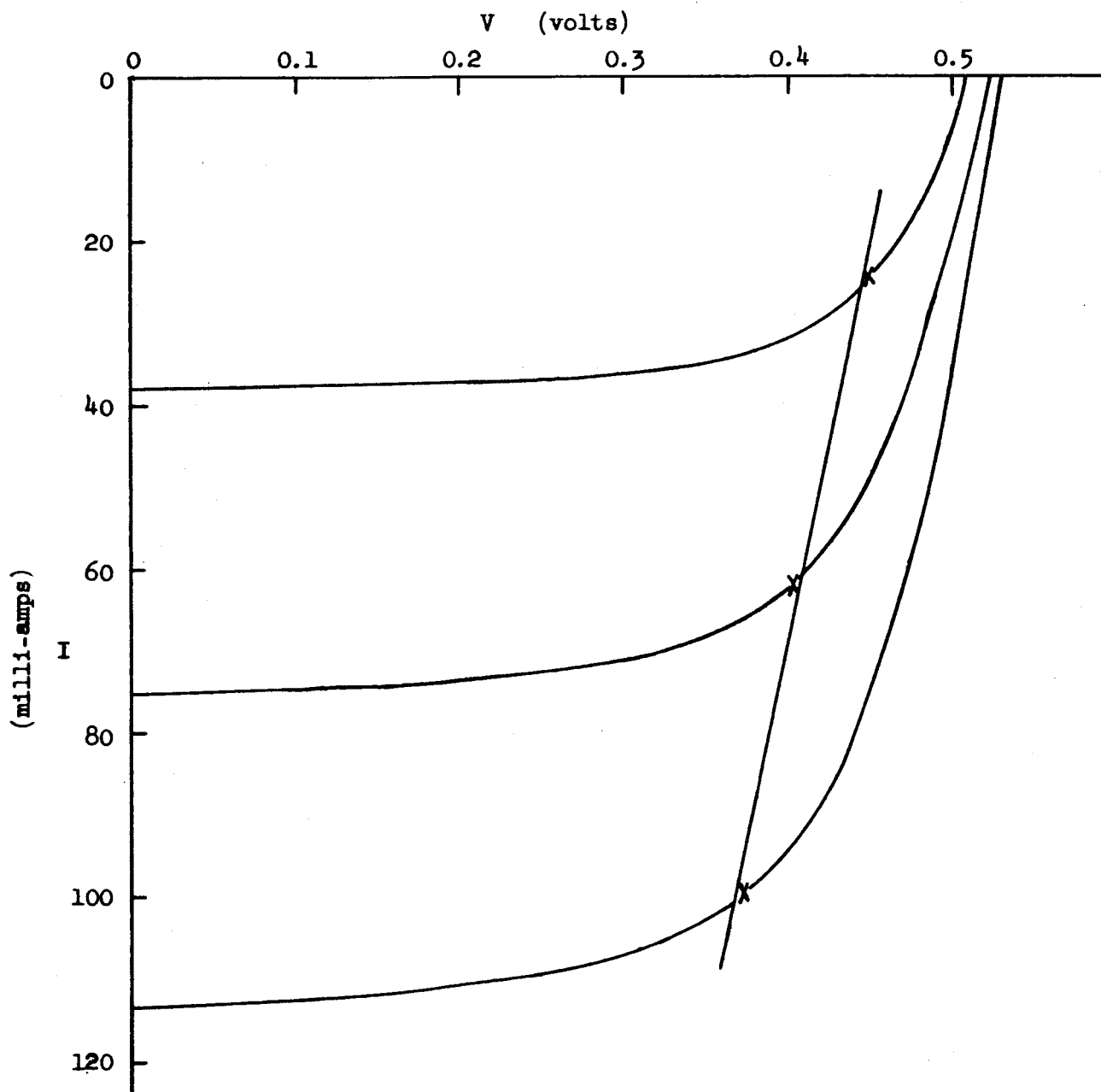
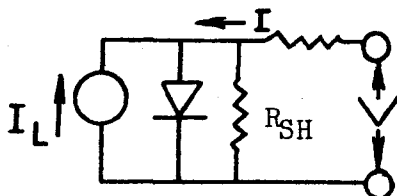


Figure
I - V CURVE at THREE INTENSITIES
for ESTIMATION of SERIES RESISTANCE

In the case shown in the Figure 7, R_s was estimated to be approximately 1 ohm. That value was also estimated from the slope at open circuit voltage on a scope trace of the I-V curve. The middle curve in Figure 7 was made under the standard light intensity and color of the routine laboratory cell tests. The effect of R_s was mathematically removed and the resulting data gave a value of A, approximately equal to 3.5.

A third model includes a shunt resistance R_{sh} :



Its I-V characteristic is conveniently expressed logarithmically:

$$\ln \left[\frac{I + I_L}{I_0} - \frac{V - IR_s}{I_0 R_{sh}} + 1 \right] = \left[\frac{q}{AkT} \right] (V - IR_s)$$

Notice that there are five parameters: I_0 , I_L , R_s , R_{sh} , and A in this equation. It is possible to shift their relative values somewhat and yet keep the theoretical curve in a narrow channel about the experimental curve.

The above discussion suggests that investigators may find different values for certain parameters depending upon how they have approached the problem.

Evaluation of the third model could proceed with the selection of five points, (V_1, I_1) , (V_2, I_2) , (V_5, I_5) from an experimental I-V curve. The I-V characteristic equation would be written for each of the points and would be solved for the five parameters. The method of successive approximations should yield values of the five parameters giving a curve which would pass close to the five selected points. The curve found in this way would represent the I-V characteristic of the cell to a degree limited partly by the accuracy with which the original points were chosen and partly by the inadequacies of the equivalent circuit model.

COLLECTOR ELECTRODE

During the period just prior to this contract, it was found that a much improved collector contact could be made to CdS front wall film cells

by laminating a fine mesh metallic grid in place of the hand ruled conductive silver grid. These mesh grids are electroformed from various metals in a variety of spacings of the grid lines. A typical grid has 90 lines per inch. Each line is 0.00049" wide. The transmission of the grid is 88%. The most important feature of the electroformed mesh is that, unlike a woven screen, its surface is completely flat. Therefore, contact is established completely on one surface against the barrier of the cell.

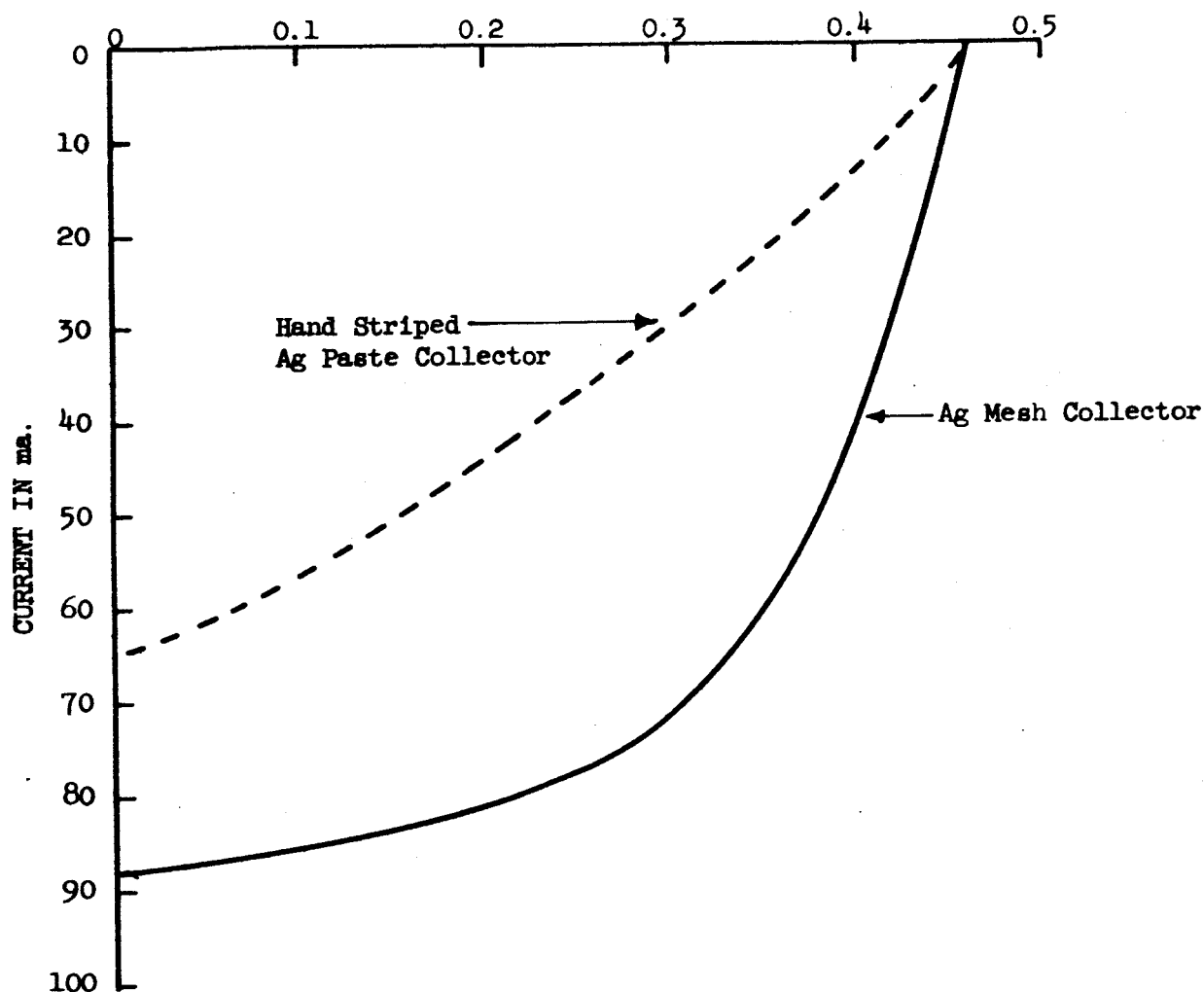
The result of this improved contact was a lowering of series resistance and an improvement in the shape of the I-V characteristic curve, as is shown in Figure 8. Thus, cell efficiencies were more than doubled in most cases.

Sheet Resistance

To determine the optimum mesh size, an attempt was made to measure the sheet resistance of the barrier. The problem was to eliminate the effect of the conducting layer of molybdenum and n-type CdS in the measurements. The electrical test circuit used for this measurement is shown in Figure 9. The average sheet resistance as measured on a number of barriers was approximately 1000 ohms per square. Since the mathematical solution of the equivalent circuit of a distributed series resistance cell involves a non-linear differential equation, an attack of the problem was made by an empirical method. The average value of sheet resistance was determined. Knowing this, an optimum electrode spacing could be calculated for any size collector electrode. At this optimum the decrease in series resistance obtained by moving the collector stripes closer together and adding a stripe would be balanced by a loss in output due to the decrease in active area covered by the extra stripe. It was determined that for a sheet resistance of 1000 ohms per square, 20 lines per inch should give the optimum grid spacing.

To corroborate this, several different meshes were tested. Various meshes were obtained, from 5 lines per inch to 1000 lines per inch. Using special testing equipment to hold the mesh against the barrier, the various grids were compared directly by testing the same cells with different grids. Four cells were used. The results appear in Table VII. The screens are listed in the order they were tested. During the tests, because of the pressures exerted against the cells, there was about a ten percent loss in efficiency.

The 90 lines per inch silver grid gave the highest output on all four cells. The 5 and 1000 lines per inch gold meshes were markedly worse than the rest in each case. The remaining grids gave somewhat lower efficiency than the 90 lines per inch silver, but were bunched more or less as a group. In Table VIII, the grids listed in Table VII have been rearranged in order of decreasing efficiency for each of the four cells tested. The grids with 25 lines per inch spacing gave sufficient output in each case to support the calculations that 20 lines per inch is adequate for contacting barriers with 1000 ohms per square sheet resistance. Even though 25 lines per inch is fifth, in cell X310, the second to the sixth ranking grids gave very nearly the same efficiency. The explanation for cell X309 is not very clear. From the I-V curves, it appeared that this cell had a



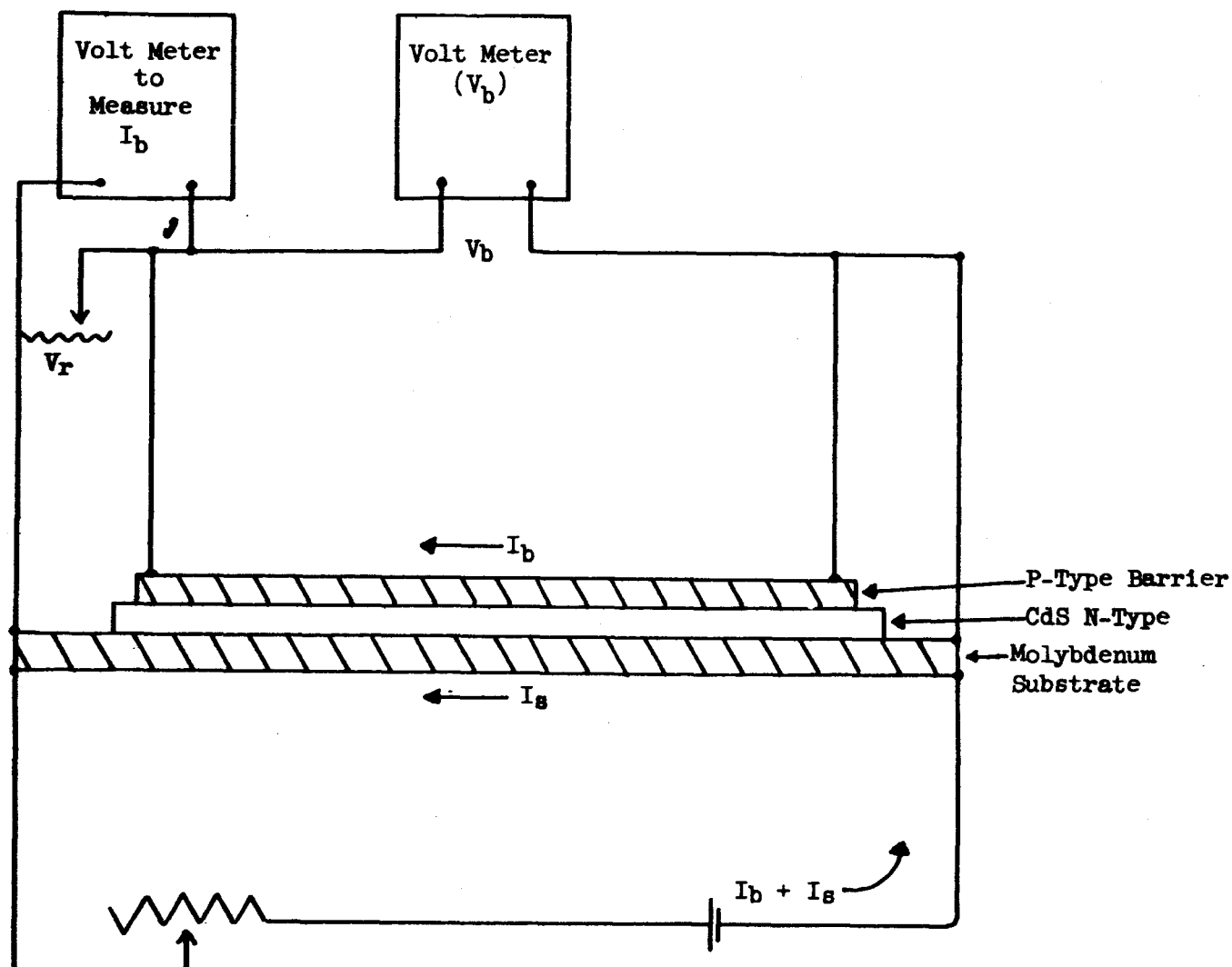
Cell X-14 CdS on Molybdenum Substrate

Illumination = $100\text{mw}/\text{cm}^2$

Collector	OCV	SCI	Area	Efficiency
Ag Paste	0.46 V	65 ma	11.9 cm^2	0.8%
Ag Mesh	0.46 V	88 ma	11.9 cm^2	1.86%

FIGURE 8

I-V CHARACTERISTIC CURVES FOR CELL X-14
WITH DIFFERENT COLLECTOR GRIDS



I_b = Current through barrier layer

I_s = Current through molybdenum substrate

V_b = Voltage across barrier layer

V_R = Voltage across current measuring resistor

Necessary condition $V_b \gg V_R$

FIGURE 9

ELECTRICAL TEST CIRCUIT FOR MEASUREMENT OF BARRIER SHEET RESISTANCE

TABLE VII

COMPARISON OF VARIOUS MESHES AS COLLECTOR ELECTRODES

Grid Material	Lines/Inch	Transmission	Eff. on Cell X300	Eff. on Cell X309	Eff. on Cell X310	Eff. on Cell S290
Au	70	88	1.35%	1.84%	1.76%	2.1%
Au	25	83	1.38	1.41	1.74	2.45
Au	1000	45	0.6	0.89	0.66	1.26
Au	90	84	1.34	1.74	1.76	2.3
Cu	70	90	1.3	1.56	1.77	2.3
Ni	70	90	1.29	1.77	1.71	2.4
Ag	90	88	1.5	2.24	2.19	2.71
Ag	280	69	1.07	1.76	1.56	2.08
Au	70	88	1.19	1.64	1.5	2.28
Au	5	98	0.76	0.68	0.71	1.12
Ag	70	88	1.26	1.7	1.65	2.36

Areas of all grids were approximately the same (About 14 cm^2).

TABLE VIII

MESH COLLECTORS FROM TABLE VII LISTED ACCORDING TO EFFICIENCY

RANK	CELL X300	CELL X309	CELL X310	CELL S290
1	Ag 90	Ag 90	Ag 90	Ag 90
2	Au 25	Au 70	Cu 70	Au 25
3	Au 70	Ni 70	Au 70	Ni 70
4	Au 90	Ag 280	Au 90	Ag 70
5	Cu 70	Au 90	Au 25	Au 90
6	Ni 70	Ag 70	Ni 70	Cu 70
7	Ag 70	Cu 70	Ag 70	Au 70
8	Ag 280	Au 25	Ag 280	Ag 280
9	Au 5	Au 1000	Au 5	Au 1000
10	Au 1000	Au 5	Au 1000	Au 5

higher sheet resistance than the other three cells. This could explain the poorer performance of the 25 lines per inch mesh in this case. From the shape of the I-V curves of the other three cells it is clear that 25 lines per inch is adequate and that 5 lines per inch is inadequate for the collector. The calculations therefore seem borne out by experimental results.

It is important to note here that these tests of various collector electrodes on the special test equipment neglect the fact that for some reason the sheet resistance of the barrier region apparently increases greatly during the actual lamination process. The presence of hot flowing plastic apparently can increase the sheet resistance as much as ten fold. Probably because of this apparent increase in sheet resistance, grids with 70 to 90 lines per inch were necessary on laminated cells, though the bench tests and calculations show 20 lines per inch should be adequate.

Since it was found that more than the initial sheet resistance of the barrier was involved, the steps in the lamination were separated and the sheet resistance measured at each step. The measurements were made in air, in vacuum, over desiccant, in vacuum with heat, under pressure as experienced in lamination, and with plastic laminated to the surface. Table IX shows the results of this series of measurements. There was a large increase in apparent sheet resistance when plastic was allowed to flow under pressure against the barrier region. There was only slight increases in apparent sheet resistance under the other conditions. Exactly what was occurring is not yet clear, since the above data were not sufficient to pin down the factors involved. Perhaps the plastic was isolating small islands of the barrier region.

There was the possibility that the various mesh sizes and even the various mesh materials acted differently under the conditions of lamination. While silver was the best conductor, other metal meshes including copper, gold, and nickel were available so they were used. The results of these tests were that copper and nickel were not satisfactory, and that gold was as good or better than silver. Other tests since then have indicated that gold is the best collector for a laminated cell.

Previous experience with CdS single crystal cells indicates that all these metals should make good contact to the barrier. Therefore this test does not make sense unless some factor came into play besides contact potentials. Perhaps the gold being softer conforms to the surface better when laminated. There is also the possibility that the different screens heat up at different rates during the lamination cycle. If any got too hot, there is the possibility of floating away from the surface up into the plastic thereby producing a high contact resistance. The I-V curves of the cells with copper collectors appeared to indicate a poor contact at the collector. They displayed a very high series resistance.

Copper and silver meshes were compared on the special test equipment where the meshes were held against the barriers by air pressure. The hot flowing plastic was then eliminated from the test. The copper mesh collector was much better than when laminated. The series resistance was only slightly higher than that with the silver collectors. This may be inherent in the

TABLE IX

BARRIER SHEET RESISTANCE MEASURED WITH CELLS IN VARIOUS
AMBIENTS AND AFTER VARIOUS TREATMENTS

CELL	IN AIR	IN VACUUM	IN DESLICATED AIR	HEATED			UNDER PRESSURE	LAMINATED WITH NYLON	LAMINATED WITH KEL-F
				IN VACUUM	IN VACUUM	IN VACUUM			
588	2.13*	3.2	3.7	3.3					
642	0.73	0.87	0.53	0.36					2.26
644	0.33	0.33							
589	0.97					4.3			
627	2.10					3.5			
659	0.76					2.0			
668	0.39	0.37	0.38	0.29					2.1
669	0.73						0.65		0.68
676	0.53	0.65					0.62		0.865
679	0.60						0.67		1.62
S-7	0.93							66.5	
S-16	0.60							2.26	
S-17	0.42							2.32	

NOTES:

All resistance measurements were taken in the dark.

* All values in thousands of ohms per square.

copper, since silver is a better conductor, or it may just be due to the fact that copper is not as soft as the silver, and therefore did not conform to the barrier surface as well as the silver.

The next area to examine as a possible cause of the apparent increase is sheet resistance during lamination was the contact of the metal mesh to the barrier.

To check this area several cells were selected. First the sheet resistance was checked. The circuit used was shown in Figure 9. An important feature of the test method was an attempt to match the potential of each point on the "barrier" with the potential of the point on the substrate directly beneath it. Because of the resistance of the n-type cadmium sulfide layer between the "barrier" and the substrate, small differences in the potentials should not introduce appreciable errors in the sheet resistance measurements. Reversing the power source gave approximately the same value for apparent sheet resistance. Reversing the cell itself, in certain cases, gave a different value for sheet resistance. In some cases, the difference was as great as a factor of two. The asymmetry of the measurements for these cells probably results from large mismatches in the potential distributions of the "barrier" and the substrate.

To substantiate the method of measuring the sheet resistance, the surface of many of the cells were probed in order to get a picture of the potential distribution. The circuit used is shown in Figure 10. A "snail"⁽¹¹⁾, a small cylinder of conductive elastomer, approximately 0.1 cm in diameter was used to probe the surface. The potential distribution of the barrier of some cells was very uniform across the length of the cells. These cells had approximately the same sheet resistance when they were tested in both directions. Other cells had distorted potential distribution. These cells gave different values of apparent sheet resistance depending how they were placed in the circuit. This was probably due to localized leakage through the barrier. These cells were eliminated from the tests. The above results did indicate that the amount of mismatch in the potential distributions of the barrier and substrate in cells that give symmetrical reading is not enough to introduce appreciable error.

A number of cells with similar properties were selected. Some of the cells were laminated only over the end areas where the electrodes had been placed. Other cells were laminated over the center area and not over the electrodes. A third group of cells was laminated over the entire cell area. This procedure made it possible to separate the effects lamination causes in the barrier from those it causes at the electrodes. The values of sheet resistance measured in the cases of the first and third groups of cells changed with lamination, much more radically than in the case of the group of cells that was not laminated in the electrode area. This tended to indicate electrode effects. One of the end-laminated cells was dissected. The surface of the electrode, which had been adjacent to the "barrier", was discolored. This could have been caused by reaction of the barrier with the electrode or by an intrusion of plastic between the barrier and the electrode. Either of these things could have caused a higher resistance reading. Probing this surface of the electrode with a small conductive elastomer "snail" showed

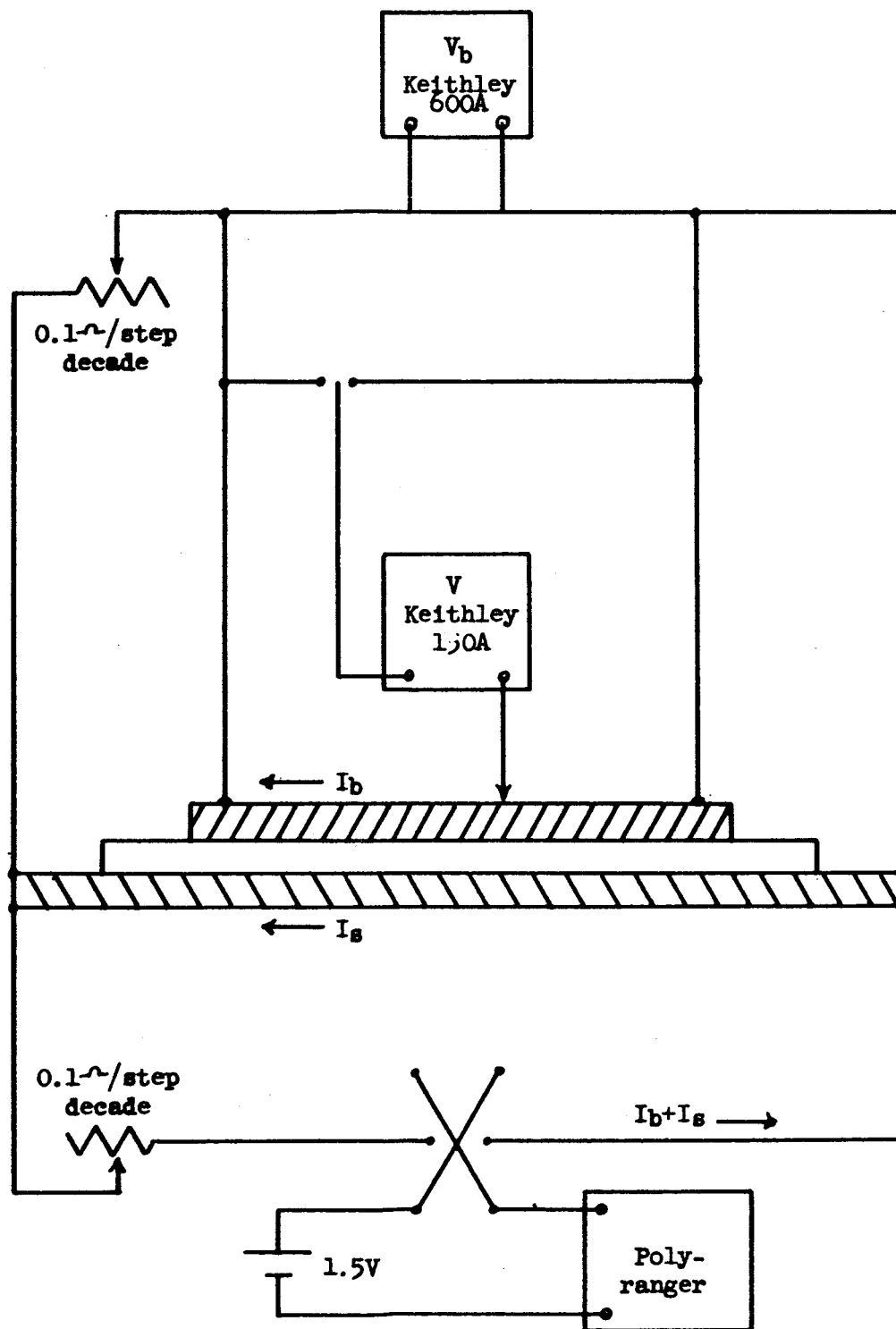


FIGURE 10

CIRCUIT TO EXPLORE THE POTENTIAL DISTRIBUTION OF CELLS

increased resistance in the discolored area.

Other tests have been run to compare the resistance between gold and silver electrodes laminated on the same cells. These tests also indicated that the increase in apparent sheet resistance was associated with the electrodes.

Recently it has been found that this is not a constant problem. In fact, many times when cells are laminated there is very little change in the apparent sheet resistance. At other times there are great changes.

Since the gold grid is only held to the surface by the nylon, and there is evidence that the grid does, at times, float away from the surface, steps are being taken to eliminate this method of contacting the barrier. This also explains why 70 or 90 lines per inch collectors must be used to get consistently good laminated cells when 20 lines per inch should be adequate. Steps are being taken to get a tighter control on the conditions of lamination. Work is also being done to eliminate the need for lamination to hold the collector mesh to the surface of the barrier.

Electroforming

The gold collector grid has been successfully applied to the barrier surface by electroplating techniques. The use of a photo-resist process to provide a plating mask has resulted in high conductivity, 80% to 90% transmitting grids, bonded directly to the barrier surface. Only certain conditions of surface pretreatment and electroplating parameters have resulted in cells being unharmed by the plating process. Most of the cells fabricated in this way were 4 cm² in area, although several of 40 cm² were attempted.

Initial attempts to fabricate a collector grid in situ involved evaporating a continuous metallic film over the cell and selectively etching the film to form a grid pattern. These experiments suffered from the effect of the etch on the cadmium sulfide sub-surface, from poor photo-resist techniques, and from drastic alterations of the photovoltaic characteristics by the evaporated metal. Later experiments, with improved photolithographic work, centered on electroplating the grid through a photoresist mask. It was found that electroplated copper also drastically altered the cells saturation current and short circuit current. The final experiments, using electroplated gold, resulted in good cells only when the plating current density was kept low, and when the cells were carefully dried before and after plating. Results of one experiment, illustrating the effect of plating speed and pretreatment, are tabulated below for some 4 cm² cells:

Cell No.	Before Processing		Prebake In Dry Air	Plating Current		After Processing	
	V _{oc}	I _{sc}		Density	Time	V _{oc}	I _{sc}
965-1	0.49v	17ma	5 min @150°C	2 ma.cm. ⁻²	6 min.	0.43v	17ma.
965-2	0.50	19	4 min @150°C	0.2	60	0.48	19
965-3	0.50	17	None	0.2	60	0.47	17
965-4	0.50	18	None	2	6	0.20	4
965-5	0.50	17	5 min @150°C	0.2	60	0.45	17
965-6	0.49	19	None	2	6	0.10	1
965-7	0.50	20	None	0.2	60	0.45	17
965-8	0.50	17	5 min @150°C	2	6	0.15	1

Cells 1 to 4 were plated within a few hours after application of the photo-resist mask. Cells 5 to 8 were exposed to room air for three days after mask application and before plating.

The above results prove the feasibility of the process, especially in view of the fact that there is a possibility of improvement in nearly every stage of the process. Plated copper may prove feasible if applied at very low current densities. Large area cells, which require a grid with lower sheet resistivity, can be processed by plating for a longer period while providing a network of high conductivity bus bars.

Twenty-five lines per inch grids with 90% transmission can be formed by photo-resist techniques, and 70% transmission can be achieved with 70 lines per inch by the state of the art in this laboratory. It is expected that the transmission can be improved in the future.

In an effort to avoid attacking the thin barrier with the plating solution, an attempt was made to fabricate a rear wall cell by painting the barrier surface with an opaque silver paste, and selectively etching out a grid on the other side, in the cell's molybdenum substrate. This technique shows some promise, but it is hampered by the lack of an etchant which will remove molybdenum and not remove the CdS below. This method does have the advantage of etching from the n-type CdS side of the cell. This material is about one and one half mils thick, so that if the etching solution removes only part of the CdS it probably will not affect the cell operation. Figure 11 is a picture of an operating rear wall cell that was fabricated in this manner. It does present a handling problem since the CdS film is practically unsupported when most of the molybdenum is etched away.

CELL ENCAPSULATION

At present the complete cell package comprises the CdS film and barrier

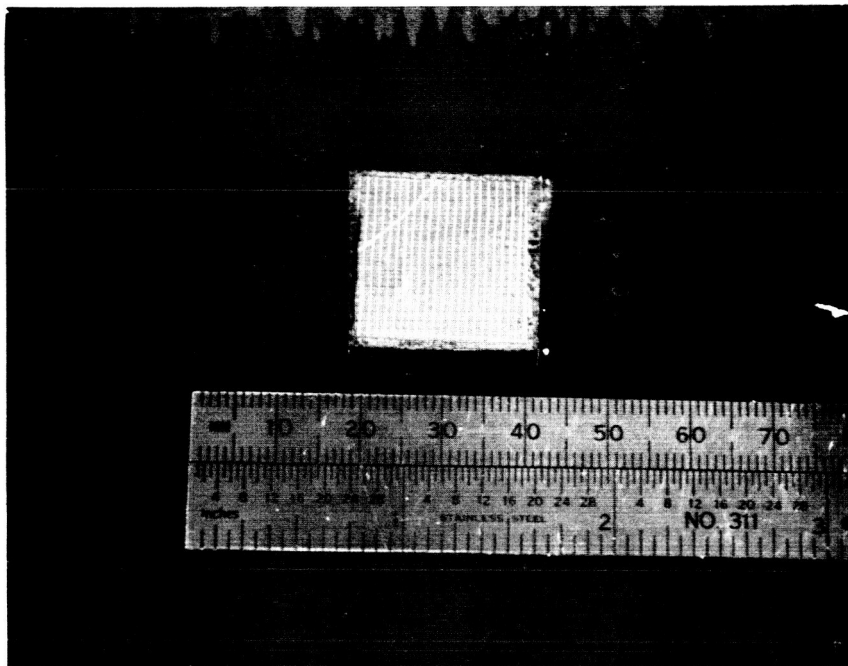


FIGURE 11
Rear Wall Cell Fabricated By
Etching Substrate

layer on a molybdenum substrate, a mesh collector, negative and positive leads, and the plastic envelope. In this section the substrate, film, barrier, and mesh are not considered. Interest is directed to the plastic, methods of encapsulation, and the lead attachment.

Plastics

Using samples supplied by Harshaw, the NASA, Lewis Laboratory performed some preliminary ultraviolet tests on the films. With this information, the data supplied by the manufacturers, and the experiences gained in this laboratory, the most favorable plastics for cell encapsulants were selected. The properties looked for in the plastics were ultraviolet, temperature, and radiation resistance. The plastic must also possess sufficient tensile properties. The three plastics that look best for space use are duPont's H-film, duPont's Tedlar, and Mylar. H-film is a polyimide, while Tedlar is a polyvinyl fluoride.

Lamination of one mil H-film to itself was not successful, and an adhesive layer of nylon had to be used. The same is true of the Mylar. No adhesive is needed for the Tedlar since it has a special heat sealable surface.

These three plastics will be compared in further tests by NASA. These tests include radiation resistance, ultraviolet resistance, thermal properties, moisture permeability, and other physical properties such as tensile strength and elastic modulus.

Encapsulation

Because of the long heating and cooling cycle used in the present lamination process, and the difficulty this causes in handling certain plastics, a new technique is being sought. The present method is too slow. The optical and physical qualities of the plastics would be less affected by a short heat and cool cycle than by the present much longer cycle. An attractive method would be impulse lamination.

Some work was initiated here on an impulse type sealer. The most favorable results have been obtained on what might be termed a "resistance heating" type system. Large amounts of electrical power are necessary for short periods of time. After several tests, it is felt that specifications for a piece of equipment including the proper power supply can now be written.

Another type of sealer that has been investigated is the heated roller type. This seals the plastics well but tends to trap vapors at the edges of the cell. There are ways that a new package could be developed employing this heated roller technique. It might also be employed in preassembling the package, e.g. putting the mesh collector on the barrier.

Miscellaneous Improvements

Results of thermal cycling tests at extreme temperatures, has made it evident that further changes are needed in the cell package. One problem area has been the cutting of the plastic by the edges of the substrate during temperature cycling. This is due to the expanding and contracting metal working against the plastic at the edge of the metal substrate. The plastic is thinned in this area during the lamination process.

To prevent any cutting of the plastic by the thin metal substrate, the corners of the substrate have been rounded and the edges sanded. A plastic picture frame of reinforcement has also been added to eliminate the thin area of plastic at the cell edges.

Still another improvement incorporated in the present package is an emissive black backing. The purpose of the black is to improve the emissivity of the package to about 0.9. Previously this black tended to chip off, now it is bonded to the plastic by heat.

Lead Attachment

One weak point in the cell package was the negative and positive lead attachment. Until now this has been a pressure contact established during the lamination process which had appeared to be satisfactory until the advent of a large number of tests.

To alleviate the problem of the pressure contacts (silver to the molybdenum, and silver to the gold mesh) separating, other precautions were taken.

In order to insure a good contact to the molybdenum substrate, a tab has been extended from one edge. This tab can be spot welded. However if it is to be soldered, it must receive additional treatment. Several attempts to plate this tab with solderable metals left much to be desired. Finally a small vacuum chamber was designed to evaporate copper on the tab after it was heated in vacuum to 500°C. This coating adheres well and can be readily soldered. The advantage is that it can be applied to the cell after the substrate is trimmed just before lamination. With this piece of equipment the tab must be about an inch long. If shorter negative leads are desired, a tinned piece of metal can be spot welded to the molybdenum tab.

There are two method of attaching the positive silver lead to the mesh. One is a thermal-compression bonding. The other is to have the lead tinned before lamination, then under the conditions of temperature and pressure of lamination, a solder joint is formed between the mesh and lead. From many tests it appears that certain fluxes must be avoided as they damage the barrier. The solder method has proven very satisfactory.

All other connections, e.g. terminals on the end of the leads, are spot welded.

These improvements insure a cell package that will not lose electrical contact under extreme temperature conditions.

PILOT LINE

During this contract a standard process line for production of CdS front wall solar cells was continually operated. This line provided a base line to evaluate advances. Periodically glass rear wall cells were also fabricated on this line to provide a continuous measure of front wall cell performance as compared to rear wall operation. The cells made on this line were used in other tests after they were evaluated, e.g. lamination experiments, life tests, etc... Several changes were incorporated into this line during this contract. For instance, at the start of the contract the collector electrode was hand striped silver conductive paint. It was later discovered that the cell efficiency could be doubled by using an electro-formed mesh collector. However, with the advent of the mesh collector, it was necessary to encapsulate each cell in order to attach the collector to the barrier. This required quite a bit more time.

In order to determine the efficiency of cells without permanently laminating them in plastic, a pressure test unit was constructed that incorporated all the features of the lamination process except the presence of the hot plastic film. This unit is illustrated in Figure 12. The cell, immediately after barrier formation, is placed in the fixture and it is clamped shut. Beneath the cell there is a rubber diaphragm. Pressure of approximately 100 psi from tank nitrogen presses the cell against a silver mesh grid and a lucite window. The cell is illuminated through the lucite window and the output of the cell measured. This allows a very close estimation of the performance of the final cell, without actually laminating a mesh against the barrier surface. The benefits of this testing method are evident. The cells can be tested and then stored in a dry atmosphere for later matching and assembly in arrays.

It was also discovered that the cells made on the pilot line were sensitive to humidity during barrier formation. The barrier was formed by electroplating Cu on the film and then heating it in air. The time of this oxidation process varied greatly. The cause was humidity variations. An electro-air dryer was installed on the oxidizing furnace. Since then the oxidizing time is easily controlled and the barriers are much more reproducible and uniform.

This pilot line has helped solve several temporary difficulties. One of the causes for the lower average efficiency was the production of less uniform films. This lack of uniformity of the films was found to be caused by a general build-up of evaporant on all the surfaces within the vacuum bell jars. Immediately after the systems were completely cleaned, the conversion efficiencies of completed cells rose sharply.

Another problem was traced to an incorrectly reading thermocouple. It appears that the vapors in the vacuum system gradually attack the thermocouples, and unless they are changed regularly they tend to give faulty readings. The thermocouples caused erroneous substrate temperature readings which resulted in many thin films. These thin films tend to develop shorts during barrier plating.

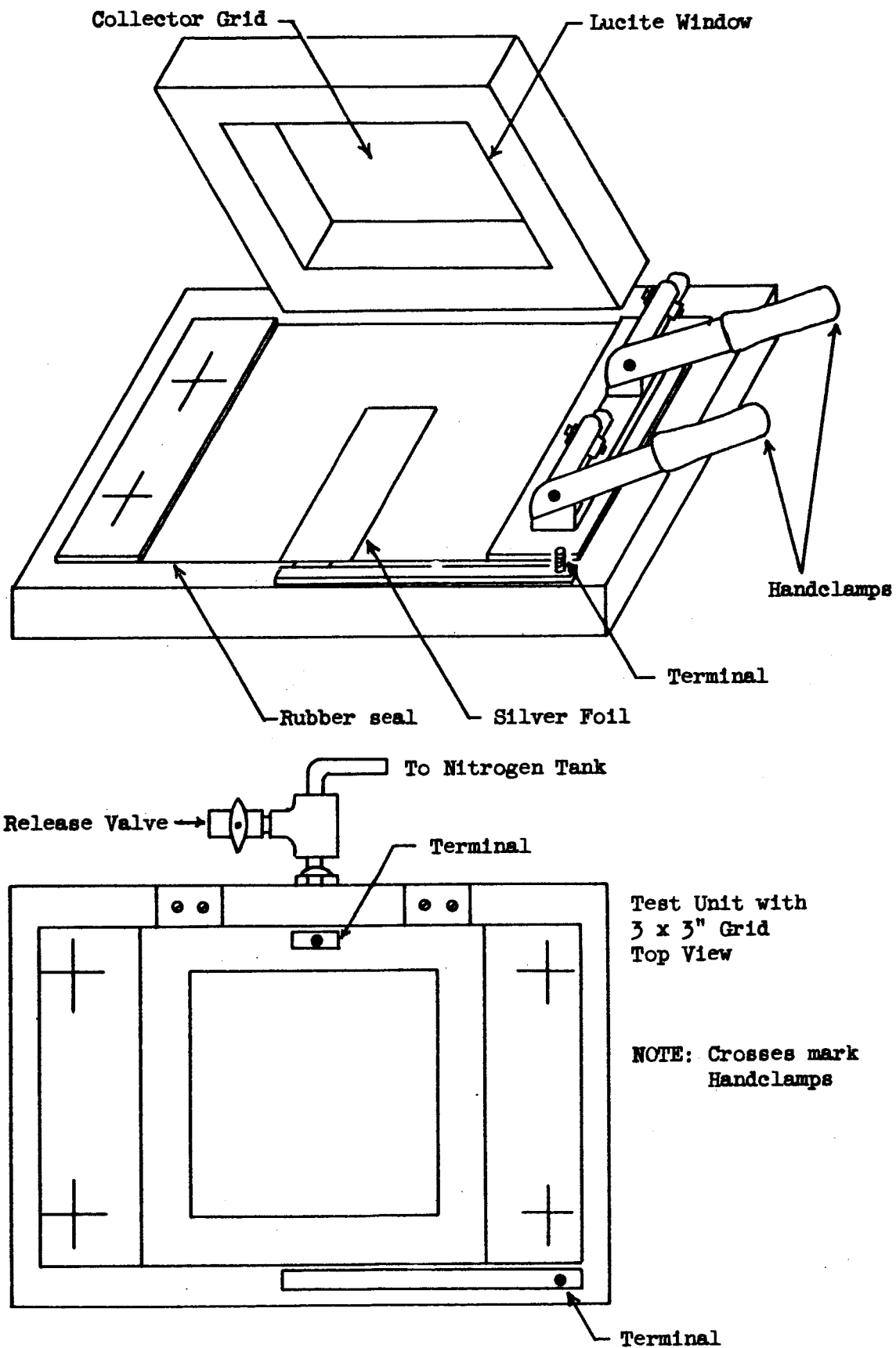


FIGURE 12

PRESSURE TEST UNIT DIAGRAM

A typical difficulty encountered was a material problem. Some of the poor cells were traced to films made from certain sinters of CdS. One lot was not completely sintered because of a power failure during the run. Other sinters displayed high oxygen contents. More rigid control of the material used for evaporation has been established as a result.

It was discovered during the pilot line operation that many cells that were considered poor, or even scrap, because of low output or apparent shorts are recoverable. The two most prevalent faults of poor cells are not due to the film formation, but to the formation of the barrier. They can be generally classified as low current output, and apparent poor shunt resistance. The cells that have low current can be recovered by simply repeating the barrier formation process without removing the first barrier. The cells that seem to have poor shunt resistance (according to the I-V characteristic) may have a very high I_0 for some unknown reason. This is demonstrated when the poor shunt characteristic disappears at liquid nitrogen temperatures. This gives an easy method of detecting this condition and separating it from true shunt problems. These cells with the possible high I_0 are recoverable by removing the barriers with potassium cyanide, and replacing them with new barriers.

Over 1000 cells were made on the pilot line during the period covered by this contract. Because of the continual changes and improvements, both the average efficiency and the maximum efficiency of the cells has increased. The highest efficiency cell produced on this line was 5.12%.

REFERENCES

1. Allen-Jones Company, Long Beach, California.
2. W. L. Bond, Notes on Solution Problems in Odd Job Vapor Coating, Journal of the Optical Society of America, Vol. 44, p. 32, June, 1954.
3. H. J. Quinn "Immersion Substrate Heater for Vacuum Deposition of Films" Rev. Sci. Instr. 32 No. 12, pg. 1410 (December, 1960).
4. F. A. Shirland, G. A. Wolff, J. D. Nixon, Fifth Quarterly Progress Report, Contract AF33(616)-7528, pg. 22.
5. J. C. Schaefer, R. J. Humrick, R. F. Belt, First Quarterly Technical Progress Report, AF33(615)-1248, pg. 2.
6. Electrodes on Cadmium Sulfide Crystals; R. H. Bube, Photoconductivity of Solids, John Wiley & Sons Inc., 1960.

Ohmic Probe Contacts to CdS Crystals, Y. T. Sihvonen & D. R. Boyd, Journal of Applied Physics 29 (8) 1143-1145 (August, 1958).

Ohmic and Rectifying Contacts to Semiconducting CdS Crystals, William C. Walker and E. V. Lambert. Journal of Applied Physics 28 (5).
7. J. C. Schaefer, R. J. Humrick, E. R. Hill, R. F. Belt, Investigation of Thin Film Cadmium Sulfide Solar Cells. ASD-TDR-63-743, November, 1963, pg. 42.
8. M. B. Prince, "Silicon Solar Energy Converters", Journal of Applied Physics, 26, pp 534-540.
9. F. A. Shirland, G. A. Wolff, J. C. Schaefer, G. H. Dierssen, ASD-TDR-62-69, Vol. II, "Research on Solar Energy Conversion Employing Cadmium Sulfide, pg. 25ff.
10. P. A. Illes, The Present Status of Silicon Solar Cells, I.R.E. Transactions on Military Electronics, Vol. MIL-6, January, 1962, pg. 11 and J. Wolff and H. Rauschenback, Series Resistance Effects on Solar Cell Measurements, Advanced Energy Conversion, Vol. 3, No. 1, April-June 1963, pg. 467.
11. Pylon Company, Inc., Attleboro, Massachusetts.